Plasmonics (2019) 14:1539–1546
https://doi.org/10.1007/s11468-019-00948-3

Center Frequency and Bandwidth Reconfigurable Spoof Surface Plasmonic Metamaterial Band-Pass Filter

Rahul Kumar Jaiswal[1] · Nidhi Pandit[1] · Nagendra Prasad Pathak[1]

Received: 7 January 2019 / Accepted: 10 April 2019 / Published online: 3 May 2019

Abstract

In this study, we report a design concept to obtain center frequency and bandwidth reconfigurable spoof surface plasmon polaritons (SSPP) band-pass filter using T-shaped spoof SPP resonator. The design, analysis, and implementation of the proposed filter have been given with detailed mathematical analysis. Tuning has been performed using varactor diode which is introduced at different positons in the T-shaped resonator. Since spoof SPP has high field confinement and enhancement, hence it offers low crosstalk and mutual coupling as compared with conventional microstrip which is desirable to make low-loss system. The filter has been fabricated using a 1.52-mm-thick microwave laminate and characterization has been done using Keysight Field-Fox analyzer N9918A. The fabricated filter has a reconfigurable center frequency from 4.2 to 4.4GHz with insertion loss ~4.2 dB and bandwidth reconfigurable from 4.12 to 4.52GHz with ~3.8 dB insertion loss in the tuning range. The proposed reconfigurable band-pass filter will pave an important role in the designing and developing of the flexible plasmonic circuits and systems.

Keywords Band pass filter · Bandwidth · Center frequency reconfigurable · Spoof surface plasmon polaritons (SSPPs)

Introduction

Band-pass filters (BPFs) are the essential front-end component for RF/microwave systems. Recent advancements in modern wireless and radar communication applications demand high-performance and dynamically controlled RF subsystems. Hence, electronically tunable microwave filters are gaining more attention for research and development. Conventional microwave filters generally use traditional microstrip technology which suffers from radiation losses, crosstalk, and mutual coupling problems. Crosstalk involves in-between transmission line results in signal integrity issues and thus limits the performance of RF systems [1]. The solution to overcome this problem lies in using spoof surface plasmon polariton (spoof SPP)-based RF systems [2, 3].

✉ Nagendra Prasad Pathak
nagppfec@iitr.ac.in

Rahul Kumar Jaiswal
rjaiswal@ec.iitr.ac.in

Nidhi Pandit
npandit@ec.iitr.ac.in

[1] Department of Electronics and Communication Engineering, Indian Institute of Technology Roorkee, Roorkee, Uttarakhand 247667, India

Natural SPP are unique surface waves that are highly localized at the interface of metal-dielectric and found at optical and near-infrared frequencies. It decays exponentially in the vertical direction of the interface hence exhibit subwavelength field confinement and enhancement [4, 5]. Since metal behaves like plasma with negative permittivity at optical frequencies, hence SPP wave is supported by the metal-dielectric interface. However, metals show characteristics like a perfect conductor (PEC) at microwave and THz frequencies. Hence, subwavelength features are usually not found at these frequency regimes. Recently, it is shown that semimetal like graphene and semiconductors also support SPPs at THz frequency naturally which enables its applications in optoelectronic devices like solar cell, graphene as sensors, and other plasmonic and nano-photonic devices [6–18]. However, to realize the SPP-like characteristics in the vicinity of the metal-dielectric interface at THz and microwave frequencies, plasmonic metamaterial [19] that are the periodically corrugated metallic surfaces with 2D hole or 1D groove has been proposed, also called as spoof or designer SPP. The dispersion curve and cutoff frequency for such a structure can be altered through its physical parameter. Thus, these structures have capability of guiding and manipulating the EM waves at subwavelength scale, which can be applied to design transmission lines [20–22], and components like filters [23–25], for the excitation of antenna [26], amplifier [27], switches [28], and

tunable filters [29–33]. In [29, 30], band-stop tunable behavior has been shown by changing the physical dimension. In [32], capacitors with different values have been introduced in between the two-unit cell through which dispersion and cutoff frequency of the low-pass filter can be tuned. However, structures demonstrated in [29–32] required manual fabrication each time with different parameter values to demonstrate tunable feature. In [33], researchers have demonstrated passband tunability of spoof surface plasmon polaritons. They have used 24 varactor diodes and 25 lumped inductors in different positions of the spoof SPP-based transmission line to control the higher and lower cutoff frequency of the filter which makes this arrangement very bulky and very complex for a practical prototype.

In this report, an electronically reconfigurable center frequency as well a bandwidth BPF is proposed using T-shape spoof SPP-based resonator through varactor diodes. Three varactors are introduced at different positions of the T-shape resonator which can be controlled individually by DC bias voltage applied across them. Transition from QTEM mode of microstrip to spoof SPP mode has been used to excite the SSPP-based T-shape resonator with coupling gap *g*. The prototype has been fabricated and measured; results have been presented for the validation of the design concept.

The organization of the paper is as follows: the theory and design principle of the reconfigurable center frequency and bandwidth band-pass filter based on the spoof SPP compact T-shaped resonator has been discussed in "Theory and Design Principle." The fabricated prototype and characterization of the designed filters has been provided in "Results and Discussion." Finally, the conclusion has been drawn in "Conclusions."

Theory and Design Principle

Design of T-Shaped Spoof SPP Resonator

The proposed T-shape spoof SPP resonator along with its even- and odd-mode equivalent circuits is shown in Fig. 1. This T-shape resonator can be interpreted as two $\lambda_g/4$ resonators coupled to each other via K-invertor implemented by stubbed SSPP transmission line section. Electrical length (in degree) and admittance (1/Ω) of two of line sections are ($\phi_1/2$, Y_1) while other one has (ϕ_k, Y_1). Each transmission line is corrugated with metal strip on it with electrical length and admittance of $\triangle\phi'$ and $\triangle Y'$, respectively. By adjusting the length of the tapped open stub, which can be longer or shorter than $\lambda_g/4$, a transmission zero can be created at a frequency lower or higher than the desired passband. Since, the length of the open stub is less than $\lambda_g/4$, hence it creates a transmission zero at upper stopband as shown in Fig. 3. As the structure of the resonator is symmetric;,it will excite multimode frequency

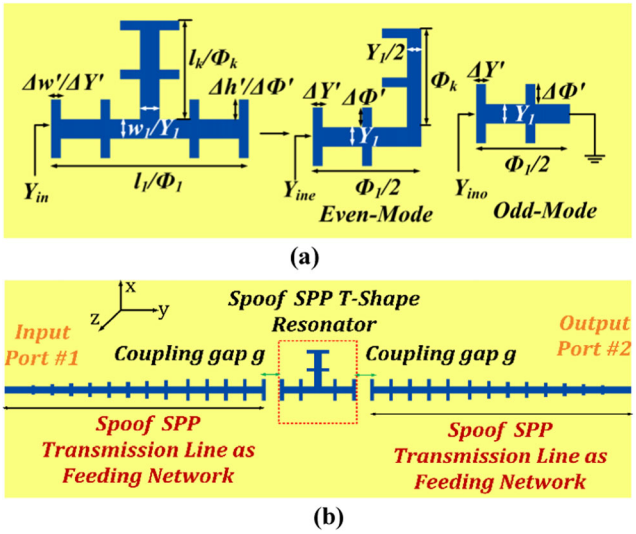

Fig. 1 Schematic of **a** proposed T-shape resonator and its even- and odd-mode equivalent circuits and **b** spoof SPP-based band-pass filter

and its operating mechanism can be explained in terms of its even-odd mode analysis.

Resonance condition for the designed resonator can be derived as:

$$Img[Y_{ine}] = 0 \tag{1}$$

where Y_{ine} is the even-mode admittance and expressed as:

$$Y_{ine} = Y_1\left[\frac{Y_M + jY_1\tan(\Phi_1/2)}{Y_1 + jY_M\tan(\Phi_1/2)}\right] + n^*\left(jY'\tan\Delta\Phi'\right)$$

with $Y_M = j\frac{Y_1}{2}\tan\Phi_k + m^*\left(j\Delta Y'\tan\Delta\Phi'\right)$, $n = 4$, $m = 2$

and

$$Img[Y_{ino}] = 0 \tag{2}$$

where Y_{ino} is the odd-mode admittance and it is defined as:

$$Y_{ino} = \left(-jY_1\cot\left(\frac{\Phi_1}{2}\right) + n^*\left(\Delta Y'\tan\Delta\Phi'\right)\right.$$

where Y_{ine}, Y_{ino} are the even- and odd-mode admittances.

From Eqs. (1) and (2), it is clear that Φ_1 affects both the even and odd modes while Φ_k influences even mode only. Hence, by tailoring the physical length the equivalent electrical path for different even and odd modal frequencies can be changed.

Design of Feeding Network

The proposed T-shape SSPP resonator is directly coupled with spoof SPP transmission feed line at input and output as shown in Fig. 1b. This transmission line consists of periodical array of unit cell as shown in the inset of Fig. 2a. The behavior of the

spoof SPP has been given by its dispersion diagram as shown in Fig. 2a in which the blue-colored line is the propagation wave vector (k_0) for the freely propagation wave and the green-colored curve is the propagation wave vector (k_y) for the spoof SPP unit cell. The propagation characteristics of the guided modes of the SSPP can be controlled by its structural parameters, which are the separation between two grooves d, groove height h, thickness of metal t, and lattice constant p. The dispersion characteristics of the spoof SPP unit cell have been analyzed through numerical simulation using CST MWS. Since k_y deviates from k_0, hence there is a mismatch of momentum and polarization between them. This mismatch leads to bad efficiency hence a conversion region needs to be designed which is fulfilled by the gradual conversion as shown in the inset of Fig. 2b, in which the height of the groove has been varied from h_1–h_8 (*0.25* to *2* mm) with equal step of h_0 (0.25 mm). The optimized structural parameters of the proposed unit cell are as follows: w = 2 mm, h = 4 mm, d = 4 mm, a = 1 mm, and p = 5 mm. Dielectric substrate having dielectric constant of 3.2, loss tangent of 0.0024, and a height of 1.52 mm with a conducting ground plane has been used for analysis and implementation. CST microwave studio has been used to obtain the numerical simulations.

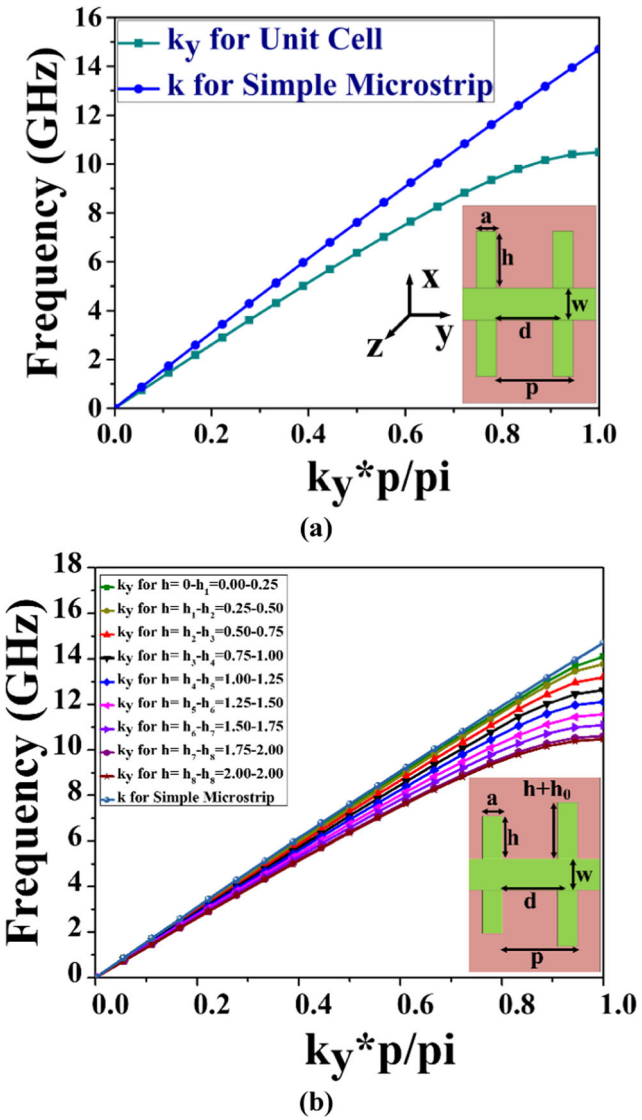

Fig. 2 Dispersion diagram **a** for double-sided grooved spoof SPP unit cell (inset: schematic of unit cell) and **b** relating the gradual conversion

Analysis of T-Shape Resonator with Different Horizontal and Vertical Electrical Length

The designed filter has a dual-mode frequency response for which parametric analysis with respect to l_1 and l_k has been done in Fig. 3a, b, respectively, to verify Eqs. (1) and (2) in EM simulation. In Fig. 3a, as we change the l_1 with l_k and all other physical parameter fixed, both the even- and odd-mode frequencies are varying hence overall center frequency of BPF

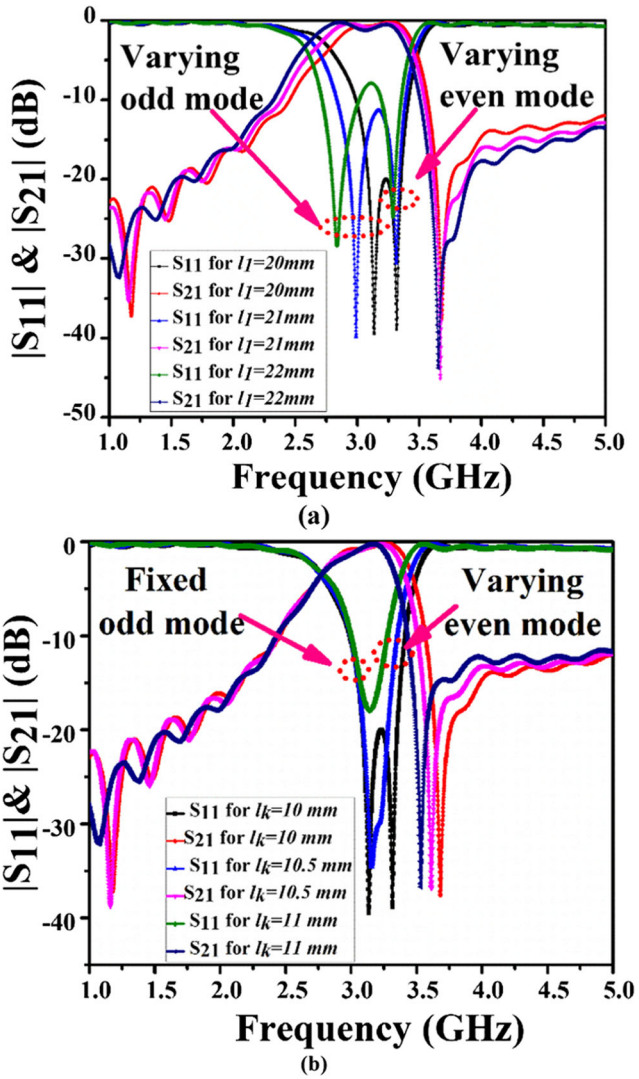

Fig. 3 Simulated *S*-parameter of the T-shape SSPP resonator–based band-pass filter with respect to change in **a** l_1 and **b** l_k

is moving towards the lower side. Similarly, in Fig. 3(b), by varying the l_k with l_1 and all other physical parameters fixed, it has been observed that the even mode is shifting towards the lower frequency side whereas the odd mode is fixed at a particular frequency. Figure 4 shows the reflection and transmission coefficient for the designed band-pass filter with different coupling gap g. It can be observed that as coupling gap increases, the input-output coupling decreases due to small value of gap capacitance and consequently a poor matching is obtained.

Design of Reconfigurable T-Shape SSPP Resonator with Even-Odd Mode Analysis

Figure 5 depicts the schematic of the proposed reconfigurable T-shape resonator along with its even- and odd-mode equivalent circuit configurations. Two varactor diodes (C) and one varactor diode (C_1) are symmetrically placed in the X and Y direction of XY plane in the resonator, respectively.

Resonance schemes for the designed resonator can be derived as:

$$Img[Y_{ine}] = 0 \tag{3}$$

and

$$Img[Y_{ino}] = 0 \tag{4}$$

where Y_{ine} and Y_{ino} are the even- and odd- mode admittance and expressed as

$$Y_{in} = Y_1\left[\frac{Y'_M + jY_1\tan(\Phi_A)}{Y_1 + jY'_M\tan(\Phi_A)}\right] + n^*\left(j\Delta Y'\tan\Delta\Phi'\right)$$

$$Yine = Yin$$

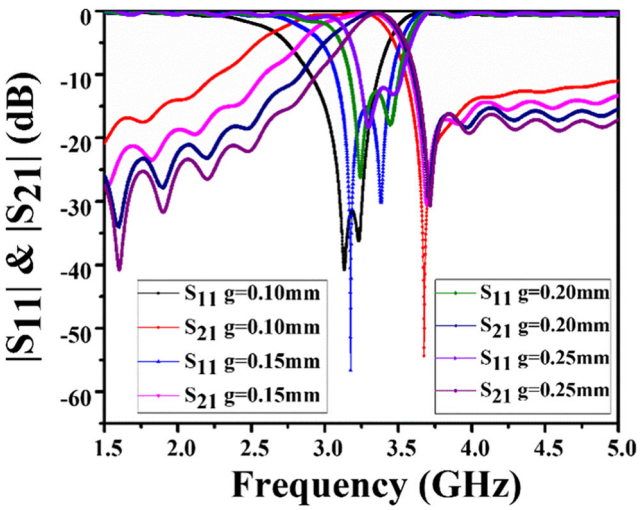

Fig. 4 Simulated S-parameter characteristics for the designed SSPP-based T-shape band-pass filter with different coupling gap g

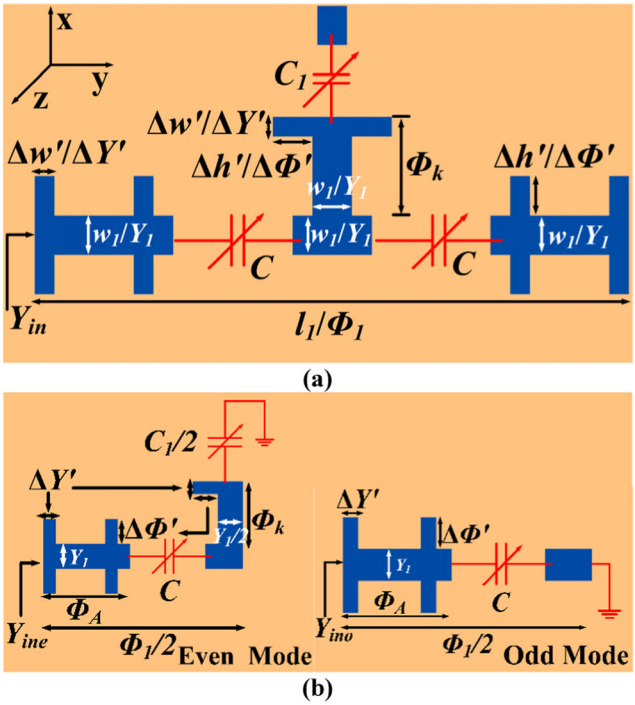

Fig. 5 Schematic of the proposed T-shape resonator with varactor diodes and its equivalent even- and odd-mode circuits

when

$$Y'_M = \frac{Y_M * j\omega C}{Y_M + j\omega C}$$

with

$$Y_M = \frac{Y_1}{2}\left[\frac{j\omega C_1/2 + j\frac{Y_1}{2}tan(\Phi_k)}{\frac{Y_1}{2} + j\left(j\omega C_1/2tan(\Phi_k)\right.}\right] + \left(j\Delta Y'\,tan\Delta\Phi'\right)$$

$$Y_{ino} = Y_{in}$$

when

$$Y'_M = j\omega C$$

For the given even- and odd-mode admittances, admittance matrix can be expressed as:

$$Y = \begin{bmatrix} Y_{11} & Y_{12} \\ Y_{21} & Y_{22} \end{bmatrix} = \begin{bmatrix} (Y_{ine} - Y_{ino})/2 & (Y_{ine} + Y_{ino})/2 \\ (Y_{ine} + Y_{ino})/2 & (Y_{ine} - Y_{ino})/2 \end{bmatrix}$$

Further the transmission zeros in terms of admittance parameter can be expressed as:

$$Y_{12} = Y_{21} = (Y_{ine} + Y_{ino})/2 = 0$$

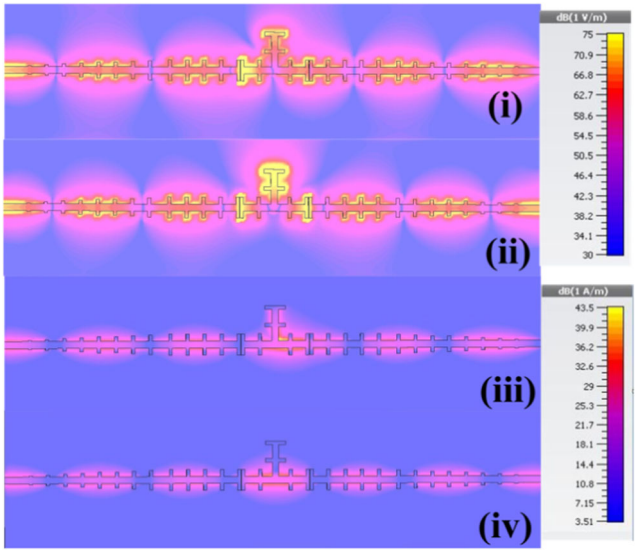

Fig. 6 (**i–ii**) E-field and (**iii–iv**) H-field distribution for designed band-pass filter at 3.23 GHz frequency

According to Eqs. (3) and (4), it can be observed that varactor (*C)* affects both the even and odd modes whereas varactors (C_1) affect the even mode only.

Figure 6 depicts the simulated E- and H-field distribution for the designed T-shaped spoof SPP resonator–based BPF at 3.23 GHz of frequency. In the passband of the designed filter, electric field is highly confined near the resonator and allows the EM field to propagate through it.

Results and Discussions

Figure 7a, b show the layout and fabricated prototype of the proposed spoof SPP-based varactor loaded tunable filter which simultaneously shows the tuning of the center frequency as well as the bandwidth. A coupling gap g = 0.12 mm has been chosen for fabricated prototype due to the fabrication tolerance.

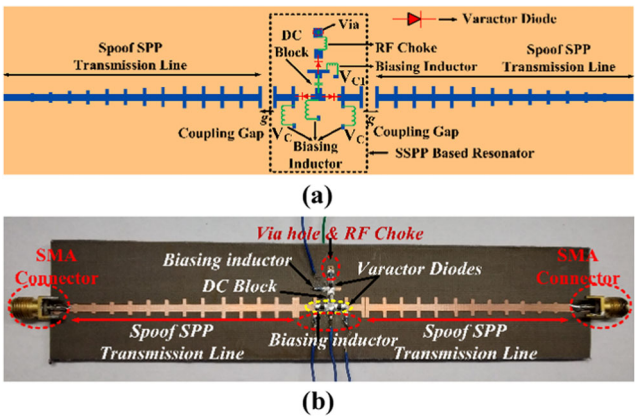

Fig. 7 **a** Schematic, **b** fabricated prototype of the proposed reconfigurable BPF

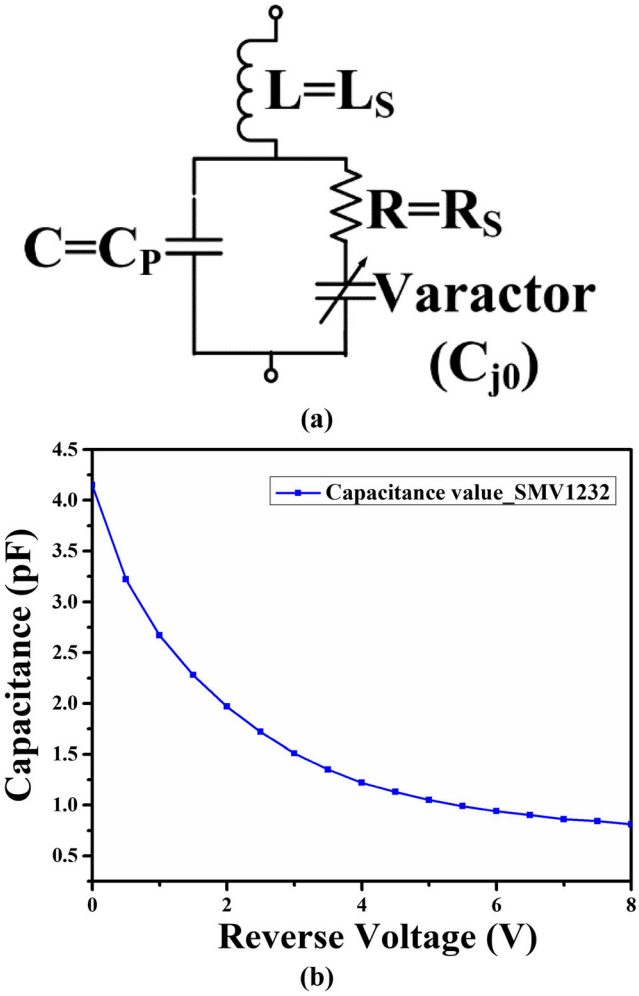

Fig. 8 **a** Model for varactor diode with C_{j0} = 3.43 pF, L_s = 0.7 nH, C_P = 0.68 pF, R_s = 1.5 Ω and **b** capacitance variation with frequency for Varactor SMV 1232 [35]

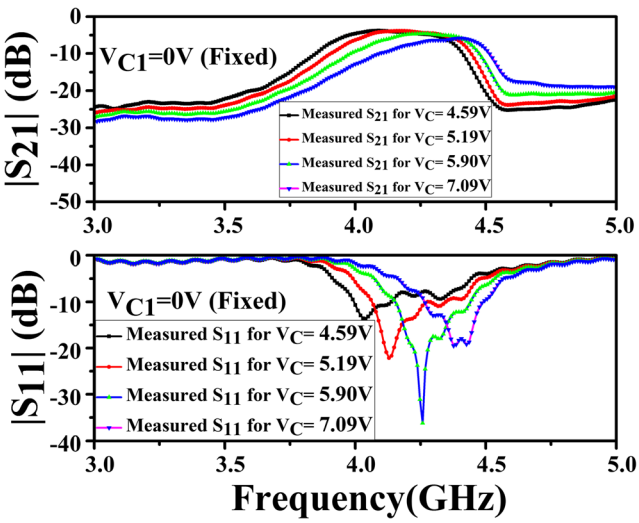

Fig. 9 Measured *S*-parameters of the proposed center frequency tunable BPF obtained with fixed V_{C1} = 0 V and varying V_C

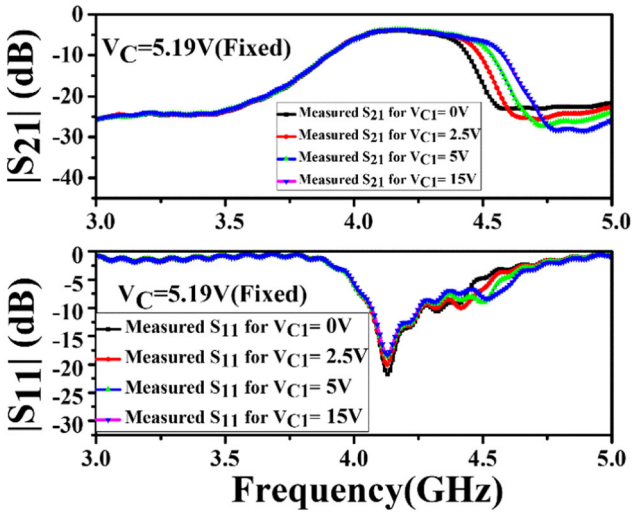

Fig. 10 Measured *S*-parameters of proposed bandwidth reconfigurable BPF obtained with $V_C = 5.19$ V and varying V_{C1}

We have chosen skyworks SMV1232-079LF as a varactor diode for our design and implementation. The simple model of a packaged varactor diode is shown in Fig. 8a. This varactor diode has junction capacitance $C_{J0} = 3.43$ pF, parasitic inductance $L_S = 0.7$ nH, parasitic capacitance $C_P = 0.68$ pF, and series resistance $R_S = 1.5\ \Omega$. Capacitance vs reverse bias voltage graph has been shown in Fig. 8b for SMV1232. It can be observed from Fig. 8b that as bias voltage increases, the junction capacitance decreases. In hardware prototype, the *SMV1232-079LF* package is used as a variable capacitor device (C, C_1) whereas Coilcraft 33 nH inductors and ATC 100 pF capacitors are used as RF choke and DC block, respectively. Corresponding to the proposed configuration, measured results have been illustrated in Figs. 9 and 10.

Since varactor C is affecting the even and odd mode simultaneously, hence by changing the bias voltage across the varactor C, the overall center frequency of degenerative mode can be varied. It is observed from Fig. 9 that keeping the V_{C1} fixed at 0 V, when we change the bias (V_C) across the varactor diodes (C) from 4.59 to 7.09 V, the overall center frequency of the band shifts from 4.2 to 4.4 GHz (200 MHz). Insertion loss of 4.2 dB is observed during the tuning range. Figure 10 depicts the tuning of bandwidth due to the change in the bias V_{C1} across the varactor diodes (C_1) for the fixed $V_C = 5.19$ V. As C_1 affects only the even-

Table 1 Comparison of state-of-the-art

Ref.	Work done	Method/remark	Reconfigurable parameter	Tuning method	IIP3	Cost
[17]	Simple rectangular and T-shape defects have been added to the conventional mictrostrip stripline and the whole structure work as a band-stop filter	Bandwidth tuning of band stop filter has been obtained by parameter variation of the defect. (Remark: Two different structures have been characterized to show narrow and wide band-stop filter using physical parameter variation)	Bandwidth	Static tuning	Not available	High
[18]	Narrow stopband or multiple stopbands have been achieved using CPW-based metallic plasmonic waveguide and single or multiple defect structure, which support spoof SPP, respectively	Center frequency has been tuned by varying the dimension of defect unit. (Remark: Tuning has been obtained through physical parameter variation)	Center frequency	Static tuning	Not available	High
[19]	Capacitor-loaded spoof SSP has been used to achieve dispersion reconfigurability and filtering characteristics	Dispersion characteristics, cutoff frequency, and operational frequency band have been tuned just by changing the capacitance value. (Remark: Different prototypes with lumped capacitance of fixed value have been characterized to show the tunable cutoff frequency of spoof SPP structure)	Cutoff frequency	Static tuning	Not available	High
[20]	Tunable band-pass characteristics of spoof SPP unit cell has been analyzed	Variable capacitance elements have been incorporated to the spoof SPP unit cell. (Remark: No measured result has been provided to demonstrate the tuning of band-pass characteristics)	Center frequency	Dynamic tuning	Not available	High
(This work)	Center frequency and bandwidth tunable BPF using T-shape resonator based on the concept of spoof SPP	Varactors are incorporated in T-shape resonating structure to control the even and odd-mode frequencies. (Remark: Fabricated prototype along with measured result)	Center frequency and bandwidth	Dynamic tuning	28.5 dBm	Low

mode wave, hence degenerative mode splitting took place here and resulted in bandwidth tuning. In this case, odd-mode frequency is fixed to 4.12 GHz while even-mode frequency varies from 4.12 to 4.52 GHz. Correspondingly, − *3* dB impedance bandwidth for the proposed configuration is varying from 500 to 630 MHz (130 MHz). Insertion loss around 3.9 dB is observed due to the little loose input-output coupling because of fabrication tolerance and SMA connector losses, also, due to the finite Q value of varactors which have inherent resistance that causes losses.

Also, intermodulation analysis has been performed for the designed band-pass filter. For that, signal distortion has been investigated using a two-tone method [35]. Simulated intermodulation product has been obtained using Harmonic Balance simulation ADS around the lowest frequency f_0 of center frequency tuning range. Two tones are separated by Δf and located at frequencies, $f_1 = f_0 - \Delta f/2$ and $f_2 = f_0 + \Delta f/2$. The intermodulation product at different input power s of *0,* 10 and 15 dBm are calculated and the corresponding IIP3 for Δf = 100 KHz is obtained 27.7, 28, and 28.5 dBm, respectively, for designed reconfigurable filter. A state-of-art comparison of the proposed work is given in Table 1.

Conclusions

In this paper, simultaneous center frequency and bandwidth reconfigurable T-shape spoof SPP BPF have been designed and analyzed by incorporating varactor diodes. This configuration is further verified by measured results of a fabricated prototype. A slightly higher insertion loss is observed which may be minimized by maintaining external *Q* value with capacitance change, using high-Q varactors, low-loss dielectric material, and CPW transmission line. The developed T-shape spoof SPP resonator–based reconfigurable band-pass filter has potential application in integrated and flexible plasmonic circuits in microwave frequency regimes.

References

1. Hill DA, Cavcey KH, Johnk RT (1994) Crosstalk between microstrip transmission lines. IEEE Trans On Electromag Compat 36(4):314–321
2. Zhang HC, Zhang Q, Liu JF, Tang W, Fan Y, Cui TJ (2016) Smaller-loss planar SPP transmission line than conventional microstrip in microwave frequencies. Sci Rep 6:23396
3. Kianinejad A, Chen ZN, Qiu CW (2016) Low-loss spoof surface plasmon slow-wave transmission lines with compact transition and high isolation. IEEE Trans Microw Theory Tech 64(10):3078–3086
4. Zayats AV, Smolyaninov II, Maradudin AA (2005) Nano-optics of surface plasmon polaritons. Phys Report 408:131–314
5. Maier SA (2007) Plasmonics: fundamentals and applications. Springer, New York
6. Otsuji T, Popov V, Ryzhii V (2014) Active graphene plasmonics for terahertz device applications. J Phys D Appl Phys 47(094006):1–10
7. Joshi N, Pathak NP (2017) Modeling of graphene coplanar waveguide and its discontinuities for THz integrated circuits applications. Plasmonics 12(5):1545–1554
8. Low T, Avouris P (2014) Graphene plasmonics for terahertz to mid-infrared applications. ACS Nano 8(2):1086–1101
9. Ju L, Geng B, Horng J, Girit C, Martin M, Hao Z, Bechtel HA, Liang X, Zettl A, Shen YR, Wang F (2011) Graphene plasmonics for tunable terahertz metamaterials. Nat Nanotechnol 6(146):630–634
10. Politano A, Chiarello G (2014) Plasmon modes in graphene: status and prospect. Nanoscale 6(19):10927–10940
11. Viti L, Hu J, Coquillat D, Politano A, Knap W, Vitiello MS (2016) Efficient terahertz detection in black-phosphorus nano-transistors with selective and controllable plasma-wave, bolometric and thermoelectric response. Sci Rep 6(1):20474-1-20474-10
12. Toudert J, Serna R (2017) Interband transitions in semi-metals, semiconductors, and topological insulators: a new driving force for plasmonics and nanophotonics. Optical Materials Express 7(7):2299–2325
13. Politano A, Viti L, Vitiello MS (2017) Optoelectronic devices, plasmonics, and photonics with topological insulators. APL Materials 5(3):035504-1-035504-10
14. Viti L, Coquillat D, Politano A, Kokh KA, Aliev ZS, Babanly MB, Tereshchenko OE, Knap W, Chulkov EV, Vitiello MS (2016) Plasma-wave terahertz detection mediated by topological insulators surface states. Nano Lett 16(1):80–87
15. Agarwal A, Vitiello MS, Viti L, Cupolillo A, Politano A (2018) Plasmonics with two-dimensional semiconductors: from basic research to technological applications. Nanoscale 10(19):8938–8946
16. Joshi N, Pathak NP (2017) Tunable wavelength de-multiplexer using modified graphene plasmonic split ring resonators for terahertz communication. Photonics Nanostruct Fundam Appl 28(1):1–5
17. Joshi N, Pathak NP (2017) Modeling of graphene-based suspended nanostrip waveguide for terahertz integrated circuit applications. J Nano Photon 12(2):1–12
18. Varshney AK, Pathak NP, Sircar D (2019) Design of graphene-based THz antennas. In: Iyer B, Nalbalwar S, Pathak N (eds) Computing, communication and signal processing. Advances in intelligent systems and computing, vol 810. Springer, Singapore
19. Pendry JB, Moreno LM, Vidal FJG (2004) Mimicking surface plasmons with structured surfaces. Science 305:847–848
20. Kianinejad A, Chen ZN, Qiu CW (2015) Design and modeling of spoof surface plasmon modes-based microwave slow-wave transmission line. IEEE Trans Microw Theory Tech 63(6):1817–1825
21. Ma HF, Shen X, Cheng Q, Jiang WX, Cui TJ (2014) Broadband and high-efficiency conversion from guided wave to spoof surface plasmon polaritons. Laser Photon Rev 8:146–151
22. Zhang W, Zhu G, Sun L, Lin F (2015) Trapping of surface plasmon wave through gradient corrugated strip with underlayer ground and manipulating its propagation. App PhysLett 106:021104
23. Zhao L, Zhang X, Wang J, Yu W, Li J, Su H, Shen X (2016) A novel broadband band-pass filter based on spoof surface plasmon polaritons. Sci Rep 6:36069. https://doi.org/10.1038/srep36069
24. Jaiswal RK, Pathak NP (2016) Spoof surface plasmons polaritons based multi-band bandpass filter IEEE APMC Conference, pp 1–4. https://doi.org/10.1109/APMC.2016.7931393
25. Zhao S, Zhang HC, Zhao J, Tang WX (2017) An ultra-compact rejection filter based on spoof surface plasmon polaritons. Sci Rep 7:10576

26. Jaiswal RK, Pandit N, Pathak NP (2017) Design, analysis, and characterization of designer surface plasmon polaritons based dual band antenna. In: Springer Plasmonics, vol 13, pp 1–10
27. Zhang HC, Liu S, Shen X, Chen LH, Li L, Cui TJ (2015) Broadband amplification of spoof surface plasmon polaritons at microwave frequencies. Laser Photon Rev 9(1):83–90
28. Song K, Mazumder P (2011) Dynamic terahertz spoof surface plasmon– polariton switch based on resonance and absorption. IEEE Trans Electron Devices 58:2792–2799
29. Jaiswal R. K., Pandit N., and Pathak N. P. (2018) Spoof surface plasmon polariton-based reconfigurable band-pass filter using planar ring resonato.r Springer Plasmonics
30. Xu B, Li Z, Liu L, Xu J, Chen C, Gu C (2016) Bandwidth tunable microstrip band-stop filters based on localized spoof surface plasmons. J Opt Soc Amer B 33(7):1388–1391
31. Xu B, Li Z, Liu L, Xu J, Chen C, Ning P, Chen X, Gu C (2015) Tunable band-notched coplanar waveguide based on localized spoof surface plasmons. Opt Lett 40(20):4683–4686
32. Tang X, Zhang Q, Hu S, Kandwal A, Guo T, Chen Y (2017) Capacitor-loaded spoof surface plasmon for flexible dispersion control and high-selectivity filtering. IEEE Microw WirelComp Lett 27(9):806–808
33. Zhang HC, He PH, Gao X, Tang WX, Cui TJ (2018) Pass-band reconfigurable spoof surface plasmon polaritons. J Phys: Cond Mat 30:134004. https://doi.org/10.1088/1361-648X/aaab85
34. Skyworks (2018) "SMV123x series: hyperabrupt junction tuning varactors," SMV123x Varactors datasheet, June 2018
35. Dussopt L, Rebeiz G (2003) Intermodulation distortion and power handling in RF MEMS switches, varactors and tunable filters. IEEE Trans Microw Theory Tech 51(4):1247–1256